

Using a Snow Drift Model to Simulate Eolian Drift and Snowfall on the Summit of Mauna Kea, Hawaii

Authors: Eaton, Leigh Anne, and Businger, Steven

Source: Arctic, Antarctic, and Alpine Research, 46(4) : 719-734

Published By: Institute of Arctic and Alpine Research (INSTAAR),
University of Colorado

URL: <https://doi.org/10.1657/1938-4246-46.4.719>

BioOne Complete (complete.BioOne.org) is a full-text database of 200 subscribed and open-access titles in the biological, ecological, and environmental sciences published by nonprofit societies, associations, museums, institutions, and presses.

Your use of this PDF, the BioOne Complete website, and all posted and associated content indicates your acceptance of BioOne's Terms of Use, available at www.bioone.org/terms-of-use.

Usage of BioOne Complete content is strictly limited to personal, educational, and non - commercial use. Commercial inquiries or rights and permissions requests should be directed to the individual publisher as copyright holder.

BioOne sees sustainable scholarly publishing as an inherently collaborative enterprise connecting authors, nonprofit publishers, academic institutions, research libraries, and research funders in the common goal of maximizing access to critical research.

Using a snow drift model to simulate eolian drift and snowfall on the summit of Mauna Kea, Hawaii

Leigh Anne Eaton* and
Steven Businger*†

*Department of Meteorology,
University of Hawaii at Mānoa, 2525
Correa Road, Honolulu, Hawaii 96822,
U.S.A.

†Corresponding author:
businger@hawaii.edu

Abstract

The goal of this research is to help develop a better understanding of the micro-meteorology of the Mauna Kea summit area and its relationship to the distribution and population health of the Wēkiu bug (*Nysius wekiuicola*). SnowModel, a spatially distributed snow-evolution model, is used to construct snowfall and summit eolian debris (known as bug fall throughout this study) accumulation maps across the summit. Eight weather stations associated with astronomical observatories on the summit ridges and four Davis weather stations located in various cinder cones (pu'u in Hawaiian), provide the meteorological observations needed as input to run SnowModel. Snow depth observations taken after a passing cold front in January 2011 are used to help validate the model accumulation predictions prior to the climatological study. Observations from summit weather stations over a three-year period (2008, 2009, and 2010) are used as input for the modeled summit accumulations of snowfall and bug fall presented in this study. For the snowfall maps, only weather data from days during which snow fell are included. For the bug-fall estimates, all days where valid weather data are available are included in the model output. Since there are no comprehensive data available on the distribution of bug fall, the bug-fall maps only provide a climatological pattern, without reference to the magnitude of the bug fall.

The greatest modeled snow accumulations are found on Pu'u Wēkiu and Pu'u Haukea. Similar results are found in the climatological bug-fall accumulation pattern. Prevailing wind direction is most critical for the distribution of snowfall and bug fall, with maximum accumulations occurring on the lee side of ridges and crests. Favorable Wēkiu bug trapping sites in which bugs were found historically are spatially well collocated with snowfall and bug-fall accumulations, suggesting that the results of this study will be of interest to entomologists in locating Wēkiu bug populations.

DOI: <http://dx.doi.org/10.1657/1938-4246-46.4.719>

Introduction

Mauna Kea is a dormant post-shield volcano located on the Big Island of Hawaii. The summit rises 4205 m above sea level and sits well above the typical trade-wind inversion (~2255 m) that limits depth of clouds and convection within the island chain (Cao et al., 2007). The timberline sits just higher, at ~2895 m. Therefore, the summit is classified as semi-arid alpine tundra. At the summit, air temperatures are cool to cold, with nocturnal freezing throughout the year, and extremely dry dew-point temperatures that result in a very low density of vascular plants (James, 1922; Hartt and Neal, 1940; Ugolini, 1974; da Silva, 2012).

The arid climate and low incident angle of the sun on some aspects of the Mauna Kea summit result in average soil temperatures below freezing for extended periods (Ehse, 2007). Areas of permafrost were discovered in 1969 near the lowest point in the crater of Pu'u Wēkiu (Woodcock, 1974). Woodcock suggested that the permafrost was facilitated by nocturnal pooling of cold air on wind still nights. More recently, Ehse (2007) measured soil temperatures in the summit area. Ehse found mean temperatures below freezing and near surface ice at several locations that she surveyed from mid-January to early March. By virtue of their limited duration, Ehse's observations do not confirm the presence of permafrost. However, they are still relevant to this study. It is suggested that the soil sites that Ehse identified as having sub-freezing temperatures for long periods of time are not sites where significant Wēkiu bug populations would likely be found owing to

unfavorable conditions for growth of juvenile Wēkiu bugs (Eiben and Rubinoff, 2010).

Aside from prevailing trade winds, the summit does experience a variety of weather systems, including kona lows, upper-level lows, tropical upper-tropospheric troughs, and the rare tropical cyclone (Blumenstock and Price, 1967; Worthley, 1967; and Kodama and Businger, 1998). These weather systems bring clouds and rain and snow to the summit. Average wind speed at the summit is approximately 4–5 m s⁻¹, with much higher winds during the passage of storms (Bely, 1987; da Silva, 2012). Consistent with the nature of post-shield volcanoes, the slopes of Mauna Kea are generally smooth and gradual (on average 7%–12% grade). However, on the summit, slopes of 30% can be seen on the flanks of various pu'us. Pu'us are cinder cones that were created from explosions of highly vesicular material such as ash, lapilli, and cinder. The ash was carried downwind, and the lapilli and cinder fell close to the explosion site forming the cinder cones (Porter, 1997). The current day geological make-up of the summit area includes an array of pu'us, glacial till, dikes, various lava flows, and glacial outwash (Wolfe et al., 1997; Sustainable Resources Group International, 2009).

Although the summit is considered to be a harsh alpine tundra, it is not entirely void of plant and animal life. Summit flora includes lichens, mosses, bryophytes, low shrubs, rosette plants, and small diffuse herbs. The summit is also a habitat for a multitude of arthropods, including spiders, moths, mites, spring-tails, centipedes, and true bugs (Group 70 International, 2007). Several early studies focused on the distinct ecology of Mauna Kea (Bryan,

1923, 1926; Papp, 1981; Guppy 1987). Guppy (1897) stated that “insects of various description are common on the summit. One species of butterfly common at the coast is not at all infrequent. The butterflies were more common to be found dead than alive, and those flying around about were in a half drowsy condition and easily caught.” He went on to say, “No doubt they had been brought up to this absolutely sterile region by the wind. Evidently, most if not all of the butterflies and moths soon die, and probably the other insects, too. The whole matter is, however, very suggestive, and shows how readily insects (even the parasitic bug) may find their way into the upper air currents.” Bryan (1923, 1926) described the similar species and their basic behaviors that are found at the higher elevation sites of Mauna Kea and Mauna Loa. Their studies preceded the finding of the Wēkiu bug by several decades but have helped to describe how life on the summit is sustained. Swan (1963) introduced the term *aeolian ecosystem*, which describes a habitat that is solely dependent on the transport of nutrients (biological fallout such as organic debris and insects) by the wind and applies to Mauna Kea.

The Wēkiu bug (*Nysius wekiuicola*) has been a focus of research since its discovery in 1980 by biologists searching for insects near the Canada, France, and Hawaii Telescope (CFHT) (Ashlock and Gagne, 1983). This true bug is endemic to the summit and receives its nutrients and moisture from the distribution of eolian debris and snow (Englund et al., 2002, 2009; Eiben and Rubinoff, 2010; Fish and Wildlife, 2010). Early entomology studies have shown that the Wēkiu bug is active in the winter and is commonly found in and adjacent to snowpack areas (Ashlock and Gagne, 1983).

Although it is located in the tropics, the summit of Mauna Kea can and does receive snowfall. There are no formal studies detailing the climatology of snowfall events for the summit because of the limited snow depth and snowfall data. However, da Silva

(2006) created a proxy, where observations of temperature and relative humidity are below 0 °C and greater than 80%, respectively, for periods of 4 hours or more, to estimate the average number of snowfall events per month. She found that January typically has six such events, February and March both averaged five events, and November averaged four. In 2008, the summit experienced 40 days where there was recorded precipitation and temperatures below 0 °C at one or more of the weather stations. In 2009, the summit experienced 52 days like this (Fig. 1).

How wind flow varies over terrain has been widely studied (e.g., Jackson and Hunt, 1975; Whiteman, 2000). It is known that wind speed, direction, and associated turbulence all change as air flows over sloped terrain. Unstable and neutrally stable air is more easily carried over a hill or pu'u. For stable air, the degree of stability, wind speed, and terrain characteristics determine how the protruding pu'u affect the flow. These variables are combined into the Froude number, which can be used to diagnose the behavior of the flow. The highest wind speeds in flow around a barrier are on the sloped sides where flow follows the terrain contours. In this study, the analysis is restricted to the micrometeorology of the summit region itself (Fig. 2).

This study uses SnowModel (Liston and Elder, 2006b), a spatially distributed snow evolution model to create climatological distributions of snow and bug fall. A description of SnowModel is given in the next section. The results of SnowModel include estimates of the distribution of snowfall and eolian debris (bug fall), which are presented in the Results section.

The main scope of the study is to focus on climatology of wind-driven moisture and nutrient sources, individually. Snowfall is the main source for water on the summit, thus wind from days meeting the snowfall proxy are used for the moisture climatology. The study assumes that eolian debris occurs throughout the year. The bug-fall distribution climatology is not limited to using wind

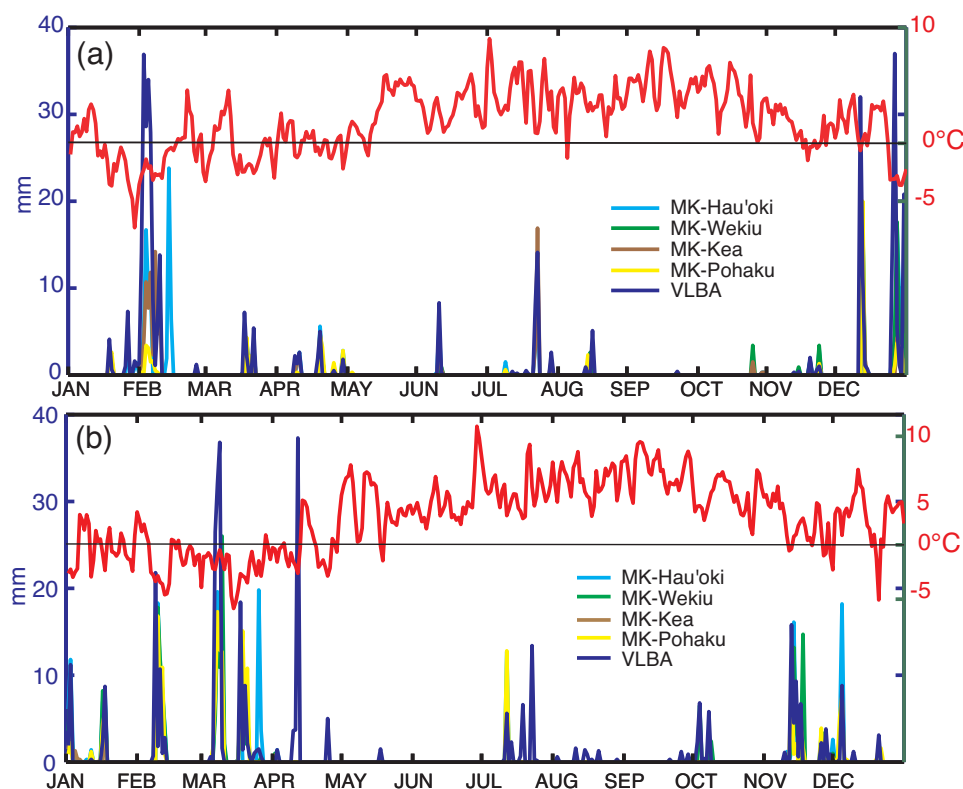


FIGURE 1. Time series of summit precipitation (mm) from listed weather stations and average daily temperature (°C, in red) from the United Kingdom Infra-Red Telescope (UKIRT) for (a) 2008, and (b) 2009.

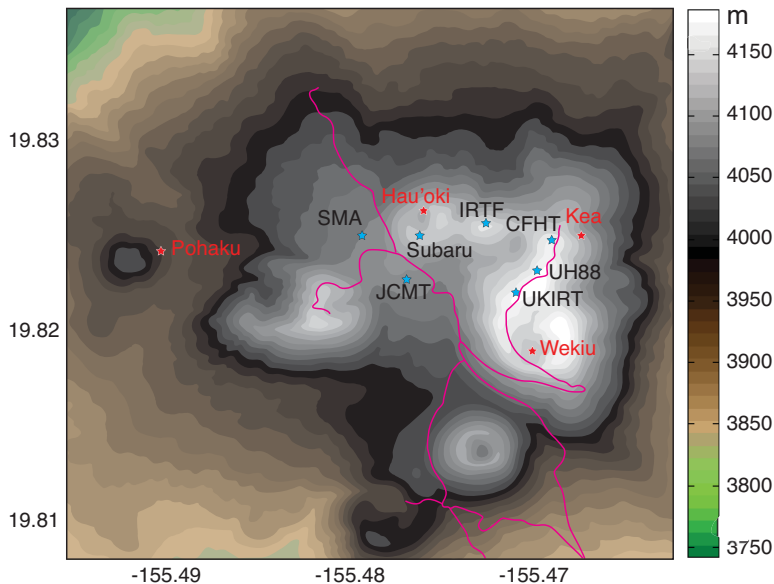


FIGURE 2. Study area spans from 19.808°N to 19.837°N and -155.495°W to -155.455°W, a 140,400 m² area. Plotted are locations of Davis weather stations (red) and telescope weather stations (blue). See Table 1 for locations and definitions of acronyms.

from only snowfall days; rather it incorporates available wind data from the entire study period. This study does not include biological data on actual transported bugs from lower elevations and/or summit bug fall.

Results will present findings separately and the concluding discussion will aim to link the multiple factors surrounding the ecology of the Wēkiu bug's habitat. The resulting climatological distributions are then compared with the locations where Wēkiu bugs have been observed in the field.

Data and Methods

This research aims to connect previous entomological and geological studies with a micro-meteorological study of the summit. Both observations and modeling are used in hopes of gaining a better understanding of the endemic Wēkiu bug's habitat.

STUDY AREA

Mauna Kea, located at 19.8°N and -155.5°W, with the summit rising 4205 m above sea level, is one of the five volcanoes that make up Hawaii Island. The study area encompasses a 4320 m by 3250 m area that includes eight cinder cones, Pu'u Lilinoe, Pu'u Mahoe, Pu'u Wēkiu, Pu'u Kea, Pu'u Haukea, Pu'u Hau'oki, Pu'u Poli'ahu, and Pu'u Pōhaku. Study domain map, location, and elevation of pu'us are seen in Figure 2 and Table 2. Elevation in the region ranges from 3741.6 m to 4205 m. The terrain comprises mainly cinder cones and glacial till. The central southern region of the domain is the northern tip of the Mauna Kea Ice Age Natural Area Reserve, which holds the Mauna Kea Adze Quarry.

The summit also houses the world's largest observatory for optical, infrared, and sub-millimeter astronomy. Presently, there are 13 active telescopes operating on Mauna Kea, several of which support basic weather stations. Additionally, four Davis weather stations were installed in 2007 in low-lying areas within four different pu'us (Hau'oki, Kea, Wēkiu, and Pōhaku) under the supervision of the Wēkiu Bug Scientific Advisory Committee (WBSAC) (Table 1).

MODEL

SnowModel is a spatially distributed snow-evolution modeling system that includes first order physics required to simulate snow evolution within each of the snow climates—that is, ice, tundra, alpine/mountain, prairie, maritime, and ephemeral (Liston and Elder, 2006b). SnowModel has been tested on a variety of snowy environments (i.e., Colorado [Greene et al., 1999], Antarctica [Liston et al., 2000], Idaho [Prasad et al., 2001], and Alaska [Liston and Sturm, 2002]).

SnowModel is composed of four sub-models—MicroMet, EnBal, SnowPack, and SnowTran-3D. MicroMet was developed by Liston and Elder (2006b) to produce high-resolution atmospheric variables (air temperature, relative humidity, wind speed, wind direction, incoming solar radiation, incoming longwave radiation, surface pressure, and precipitation), using meteorological point data from weather stations as input. The output from MicroMet is then available as input for spatially distributed terrestrial models over a wide variety of landscapes.

Included in MicroMet is a three-step preprocessor that helps to identify and/or correct deficiencies found in the station data. MicroMet uses the Barnes objective analysis scheme (Barnes, 1973; Koch et al., 1983) to interpolate irregularly distributed meteorological data to a regularly spaced grid, with corrections based on known temperature-elevation, wind-topography, and solar radiation-topography relationships (Liston and Sturm, 2006). Detailed physics are provided in Liston and Elder (2006a).

EnBal uses the near-surface atmospheric conditions produced by MicroMet to simulate surface skin temperature and energy and moisture fluxes. Surface latent and sensible heat fluxes and snow-melt calculations are made using the surface energy balance model,

$$(1 - \alpha)Q_{si} + Q_{li} + Q_{le} + Q_h + Q_e + Q_c = Q_m, \quad (1)$$

where Q_{si} is the solar radiation reaching the surface, Q_{li} is the incoming longwave radiation, Q_{le} is the emitted longwave radiation, Q_h is the turbulent exchange of sensible heat, Q_e is the turbulent exchange of latent heat, Q_c is the conductive energy trans-

TABLE 1
Weather stations and their locations, elevations, recorded variables, and valid dates for this study.

Station	Lat (°N)	Long. (°W)	Elev. (m)	T (°C)	RH (%)	WS (m/s)	WD (°)	Precip. (mm/hr)	Valid Dates
MKD Hau'oki	19.8267	-155.4753	4138	×	×	×	×	×	01/2008–03/2009 05/2009–07/2009 10/2009–7/2010
MKD Wekiū	19.8192	-155.4697	4153	×	×	×	×	×	01/2008 04/2008–04/2009 09/2009–03/2010 05/2010–,07/2010
MKD Kea	19.8261	-155.4683	4168	×	×	×	×	×	01/2008–01/2009
MKD Pohaku	19.8253	-155.4900	4003	×	×	×	×	×	01/2008–04/2008
UH88	19.8230	-155.4694	4214	×	×	×	×	×	01/2008–01/2011
CFHT	19.8253	-155.4688	4204	×	×	×	×		01/2008–07/2009 09/2009–01/2011
JCMT	19.8228	-155.4770	4075	×	×	×	×		05/3008–01/2011
UKIRT	19.8224	-155.4703	4199	×	×	×	×		01/2008–01/2011
SUBARU	19.8255	-155.4760	4163	×	×	×	×	×	01/2008–02/2008 05/2008–01/2011
VLBA	19.8014	-155.4555	4077	×	×	×	×	×	01/2008–01/2011
IRTF	19.8262	-155.4720	4168	×	×	×	×		01/2008–01/2011
SMA	19.8242	-155.4782	4080	×	×	×	×	×	01/2008–03/2008 05/2008–12/2008 07/2010–01/2011

Notes: Abbreviations in the table include Mauna Kea Davis stations (MKD); University of Hawaii 88 in. Telescope (UH88); Canada, France, Hawaii Telescope (CFHT); United Kingdom Infra Red Telescope (UKIRT); James Clark Maxwell Telescope (JCMT); Very Long Baseline Array (VLBA); Infra Red Telescope Facility (IRTF); and Sub-Millimeter Array (SMA), T = temperature, RH = relative humidity, WS = wind speed, WD = wind direction; dates are in the format mm/yyyy.

TABLE 2
Pu'us within the study area, listed from east to west from their centers.

Pu'u	Latitude (°N)	Longitude (°W)	Elevation (m a.s.l.)
Pu'u Lilinoe	19.81306	155.46222	3913
Pu'u Mahoe	19.83889	155.46389	3867
Pu'u Wēkiū	19.82361	155.47083	4205
Pu'u Kea	19.82961	155.47167	4037
Pu'u Haukea	19.81667	155.475	4008
Pu'u Hau'oki	19.82917	155.475	4045
Pu'u Waiau	19.81167	155.48111	3906
Pu'u Poliahu	19.82389	155.48444	4028
Pu'u Pōhaku	19.82694	155.49444	3952

port, Q_m is the energy flux available for melt, and α is the surface albedo (Liston and Elder, 2006b). For all of the terms found in the equation, surface temperature is the only unknown, and it is solved for. Surface temperatures greater than 0 °C indicate there is energy available for melting. The energy flux available for

melt, Q_m , is solved by setting surface temperature to zero (Liston and Elder, 2006b).

SnowPack is a simple, single-layer, snowpack evolution model that calculates snowpack changes in response to the precipitation and melt fluxes defined by MicroMet. The compaction-based snow-density evolution is based on Anderson (1976). SnowPack uses snow temperature, overlying snow weight, and the effect of snow melting to calculate temporal snow-density changes. In the case of non-blowing snow, static-surface sublimation is calculated and used to adjust the snowpack.

SnowTran-3D simulates wind-driven snow-depth evolution over topographically variable terrain (Liston et al., 1998). There are five primary components: (1) the wind-flow forcing field, (2) the wind-shear stress on the surface, (3) the transport of snow by the dominant wind-transport modes of saltation and turbulent suspension, (4) the sublimation of saltating and suspended snow, and (5) the accumulation and erosion of snow at the snow surface (Fig. 3). The required model inputs include topography, vegetation, and spatially distributed temporally variant weather data (precipitation, wind speed, wind direction, air temperature, and relative humidity).

The physics behind SnowTran-3D are primarily based on a mass-balance equation that describes the temporal variation of snow depth at each point within the simulated domain. Accumulation and erosion of snow depth at each point results from the

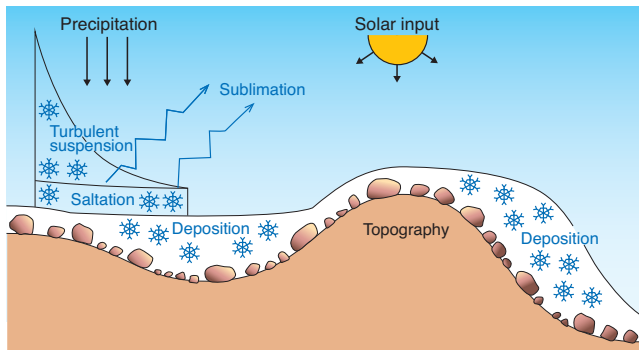


FIGURE 3. Key features of the snow-transport model (after Liston et al., 2007).

following processes: (1) changes in horizontal mass-transport rates of saltation, Q_{salt} ($\text{kg m}^{-1} \text{s}^{-1}$); (2) differences in horizontal mass-transport rates of turbulent suspended snow, Q_{urb} ($\text{kg m}^{-1} \text{s}^{-1}$); (3) sublimation of transported snow particles, Q_v ($\text{kg m}^{-1} \text{s}^{-1}$); and (4) the incoming rate of water equivalent precipitation, P (m s^{-1}). The mass-balance equation is

$$\frac{d(\rho_s \delta)}{dt} = \rho_w P - \left(\frac{dQ_{salt}}{dx} + \frac{dQ_{urb}}{dx} + \frac{dQ_{salt}}{dy} + \frac{dQ_{urb}}{dy} \right) + Q_v, \quad (2)$$

where t (s) is time; x (m) and y (m) are the horizontal coordinates in the east-west and north-south directions, and ρ_s and ρ_w (kg m^{-3}) are the snow and water densities. The mass-balance equation is solved at every time-step, for every grid cell, and is coupled with neighboring cells through spatial derivatives (Liston and Sturm, 1998).

Snow drift and accumulation totals can occur by three main modes of transport: creep, saltation, and suspension. Creep, the rolling motion of the snow along the surface, occurs in light wind speeds. SnowModel does not specifically state or calculate redistribution due to the creep process. Although, earlier snow redistribution studies have found that the percentage of redistribution from creep is small, between 6% and 10% (Kosugi et al., 1992). Saltation and suspension are the dominant processes for moving snow, and the transport rate of snow by these two methods can be described by wind speed relationships.

Saltation is the transport of snow in periodic contact with and directly above the surface; transportation rate roughly increases linearly with friction velocity (Pomeroy and Gray, 1990). Suspension, on the other hand, is the transport of snow through turbulent eddies at higher wind speeds and can occur several hundred meters above the surface. Saltation must be occurring in order to have turbulent-suspended snow particles (Liston and Sturm, 1998). Liston and Sturm (1998) showed that at higher frictional velocities, suspension is the dominant mode of transport over saltation.

For snow to be effectively transported by saltation and suspension, the snow depth must surpass the vegetation holding depth and break the gravitational and cohesive bond of the ice crystals. Vegetation holding depth is defined as the height that the snowfall accumulation must exceed to cover various surface characteristics, which may include grass, boulders, and other features blocking the snow's path. Along with exceeding the vegetation holding depth, a

threshold friction velocity (u_{*t}) must be exceeded to lift the snow for transport. The shear stress on the surface, u_* (friction velocity), produced by the wind is the main determining factor for transport. It is defined by

$$u_* = u_r \frac{\kappa}{\ln \frac{z_r}{z_0}} \quad (3)$$

where u_r (m s^{-1}) is the wind speed at reference height z_r (m), z_0 (m) is the surface roughness length, and κ is von Karman's constant. The friction velocity of a given wind must exceed a threshold friction velocity value (u_{*t}) for transport to begin. The threshold friction velocity is lower ($u_{*t} = 0.07\text{--}0.25 \text{ m s}^{-1}$) for fresh, loose, dry snow and during snowfall and higher ($u_{*t} = 0.25\text{--}1.0 \text{ m s}^{-1}$) for older, wind-hardened, dense, and/or wet snow where inter-particle bonds and cohesion forces are strong (Kind, 1981).

The loss of snow particle mass as a result of sublimation is a function of wind speed, air temperature, humidity, particle size, and solar radiation. Sublimation is the cause for significant reductions in snow mass in snow accumulation areas (Schmidt, 1982; Marsh, 1999).

To estimate the bug fall distribution on the summit of Mauna Kea, we assumed a constant bug fall rate and allowed SnowModel to determine the final bug fall distribution based on the input of wind data from January 2008 to December 2010 from the summit weather stations. MicroMet and SnowTran-3D sub-models are utilized from SnowModel. SnowPack and EnBal sub-models are turned off, to eliminate melting and density changes from energy inputs to the modeled bug fall. Within the SnowTran-3D sub-model, sublimation is removed as a valid process of transport and is set to zero. The elimination of sublimation, evaporation, and melting to the solid matter bug fall is consistent with the notion that no bug mass is lost to the atmosphere during transport or when settled. To imitate the transport of solid bug matter at the summit, temperature, relative humidity, and a bug fall precipitation rate are set to constant values of 0°C , 100%, and 0.2 mm hr^{-1} , respectively. Hypothetical stations are inserted at 10 locations around the perimeter of the study domain. These stations act to provide steady data to ingest into MicroMet. The bug fall precipitation rate (0.2 mm hr^{-1}) is a hypothetical value based on a rate that would allow for viewable model return. The results from this modeling exercise only give a relative distribution field for bug fall, but not absolute values for accumulation, since data on bug fall rates are unavailable.

Studies from Eiben and Rubinoff (2010) and Ashlock and Gagne (1983) suggest the Wēkiu bug feeds on dead or dying insects, which are wind driven and deposited on the summit from lower elevations. This study does not incorporate flight dynamics of the insects and bugs found within bug fall on the summit; we assume the majority of the incoming bug fall is dead and does not use its own means for transport or flight once it reaches the level of the study area.

Results

CASE STUDY

Initial testing of SnowModel was completed after the passage of a cold front on 11 January 2011. Between 21:30 UTC 11 January and 00:00 UTC 12 January 2011, a field experiment on the summit measured the fallen and drifted snow in Pu'u Wēkiu and Pu'u Hau'oki. The cold front dropped $\sim 15 \text{ cm}$ of snow (Fig. 4) with



FIGURE 4. Field experiment on 11 JANUARY 2011; (a) Pu'u Hau'oki during field experiment, taking snow depth measurements (Photo by C.R.S. Chambers); (b) ruler showing depth in cm (Photo by L. Eaton).

drifts up to 60 cm on the summit. Summit temperature, relative humidity, wind speed and direction, and precipitation observations from January 2011 were used as input for SnowModel (Fig. 5). The majority of the winds during the event were from the west and southwest (Fig. 5, part d).

Snow depth measurements took place between 21:30 UTC 11 January and 00:00 UTC 12 January 2011, and focused on the center depressions and the interior slopes of Pu'u Wēkiu and Pu'u

Hau'oki. The bulk of the snowfall associated with the frontal passage occurred on 10 January 2011. Output from SnowModel for 09:59 UTC 11 January 2011 shows an average depth of ~15 cm covering a majority of the summit, in good agreement with observed snow depth (Fig. 6).

The overall spatial pattern of the modeled snowfall for 10 January 2011 is in reasonable agreement with snow depth observations within Pu'u Wēkiu and Pu'u Hau'oki. Field observations show snow depth values increasing along the inner western slope of Pu'u Wēkiu, with the shallowest recordings in the center. This same spatial gradient is captured within the modeled output for Pu'u Wēkiu. However, the model does show a tendency to overestimate, especially with the depression of the pu'u, and does not extend the higher snow accumulation down the inner western slope. The inner western slope of Pu'u Wēkiu, in this case study, is considered to be the leeward side on the western crest of Pu'u Wēkiu. The buildup of snow along the upper section of the inner western slope suggests that the modeled wind speed may be dropping more quickly than is actually occurring.

Within Pu'u Hau'oki, the overall spatial pattern from the model and observations again were in reasonable agreement. In the western crease of the pu'u center, the model did a fair job in representing actual snow depths. The model underestimates the inner northern slope of the pu'u, but is in agreement with the increase in snow depth that is occurring spatially, which also holds true for the inner western slope. Pu'u Hau'oki is shielded from the south and west by other pu'us and observatories, more so than Pu'u Wēkiu. The sharp gradient found in the snow accumulation in Pu'u Wēkiu is not seen here, due to the less noticeable wind acceleration and the less steep slope within this pu'u.

Although, the overall spatial patterns from the model are in agreement with the observations, some variability in the snow depth observations not captured by the model can be, in part, attributed to the limited number of weather stations within the study domain. Additionally, subgrid-scale variability in surface terrain and roughness elements will lead to discrepancies between model and observations. The model's output resolution and $\frac{1}{2}$ arc-second National Elevation Dataset (NED) input, are not sufficient to resolve individual boulders that cause variations across the snow-depth field. GPS receivers were used to point locate the snow-depth observations, while the model uses the longitude and latitude locations from NED input.

WIND AND SNOWFALL OBSERVATIONS

Wind and precipitation data (Figs. 1, 7, and 8) are used in daily model runs to estimate the climatological accumulation of snowfall and bug fall across the summit region. Snow events are characterized by days that have precipitation and the summit average temperature is freezing or below. An overview of the wind and precipitation data is presented here. Nominally, the wind speed threshold for saltation is 5 m s^{-1} and the threshold for suspension is 15 m s^{-1} (Liston and Sturm, 1998).

Easterly winds prevail in snow events for 2008, especially in February, March, and November (Fig. 7, part a). December snow events are governed by both easterly and westerly winds; the same goes for snow events in April. The summit received snowfall 40 days out of the year for 2008 (Fig. 1, part a). The annual total snowfall observed for the year averaged over all the observation sites was 193 mm.

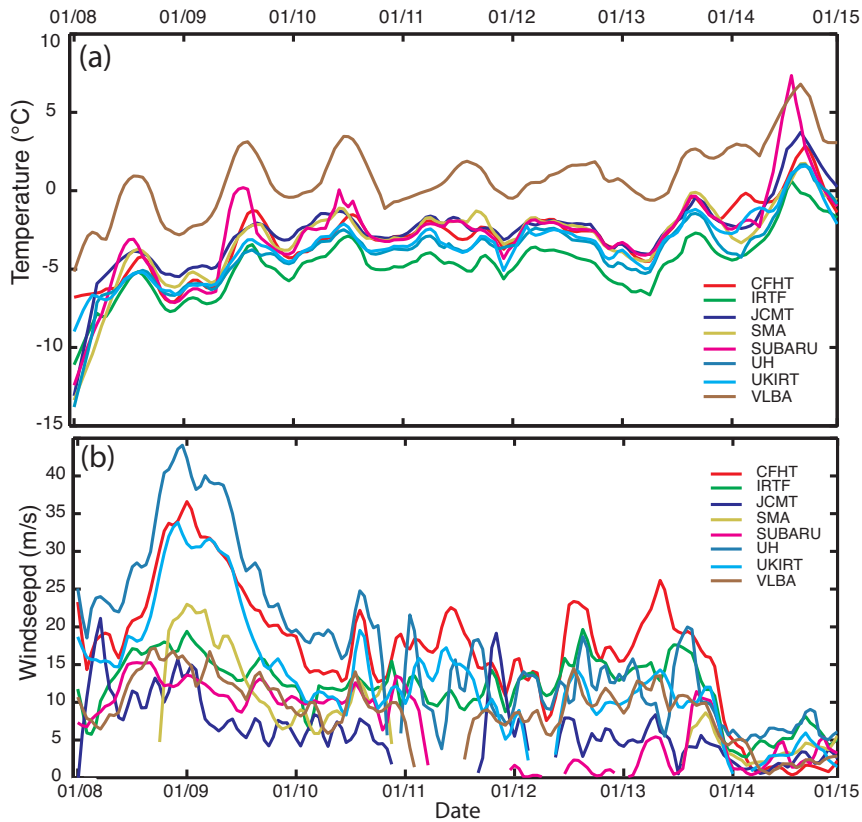


FIGURE 5. Mauna Kea summit (a) average hourly temperatures, and (b) average daily wind speed for 8–14 January 2011. (c) Precipitation time series for 12 UTC 09 January to 2300 UTC 11 JANUARY 2011. (d) Wind rose plot of Mauna Kea summit wind speeds and directions from 1000 UTC 09 January to 0900 UTC 11 JANUARY 2011. See Table 1 for definitions of site acronyms in the graph and Figure 2 for their relative locations.

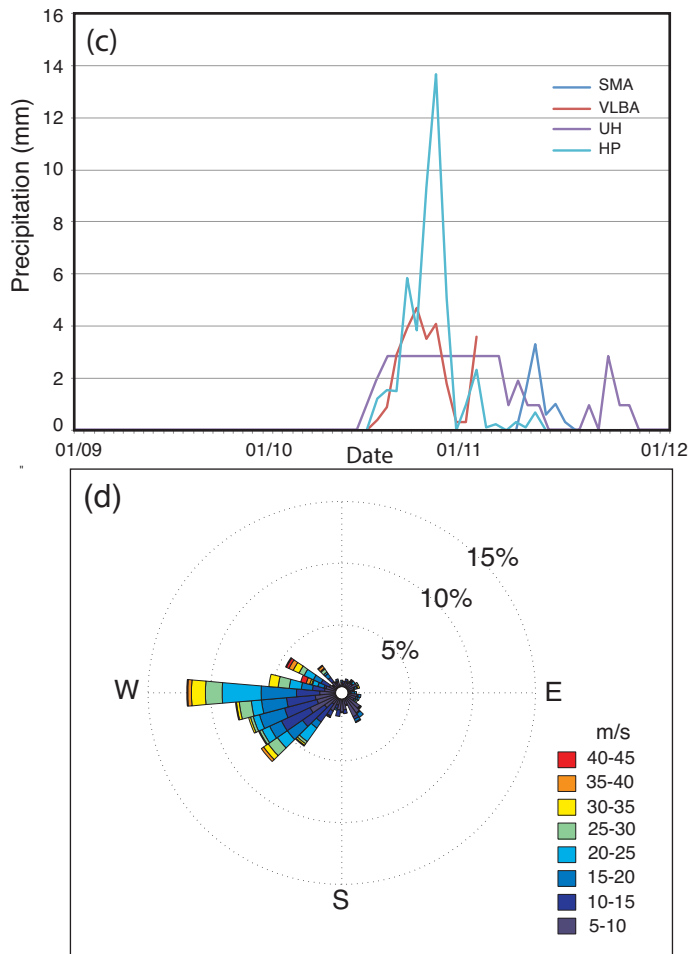


FIGURE 5. continued Mauna Kea summit c) Precipitation from 1200 UTC 09 January to 2300 UTC 11 JANUARY 2011. d) Wind rose plot of Mauna Kea summit wind speeds and directions from 1000 UTC 09 January to 0900 UTC 11 JANUARY 2011.

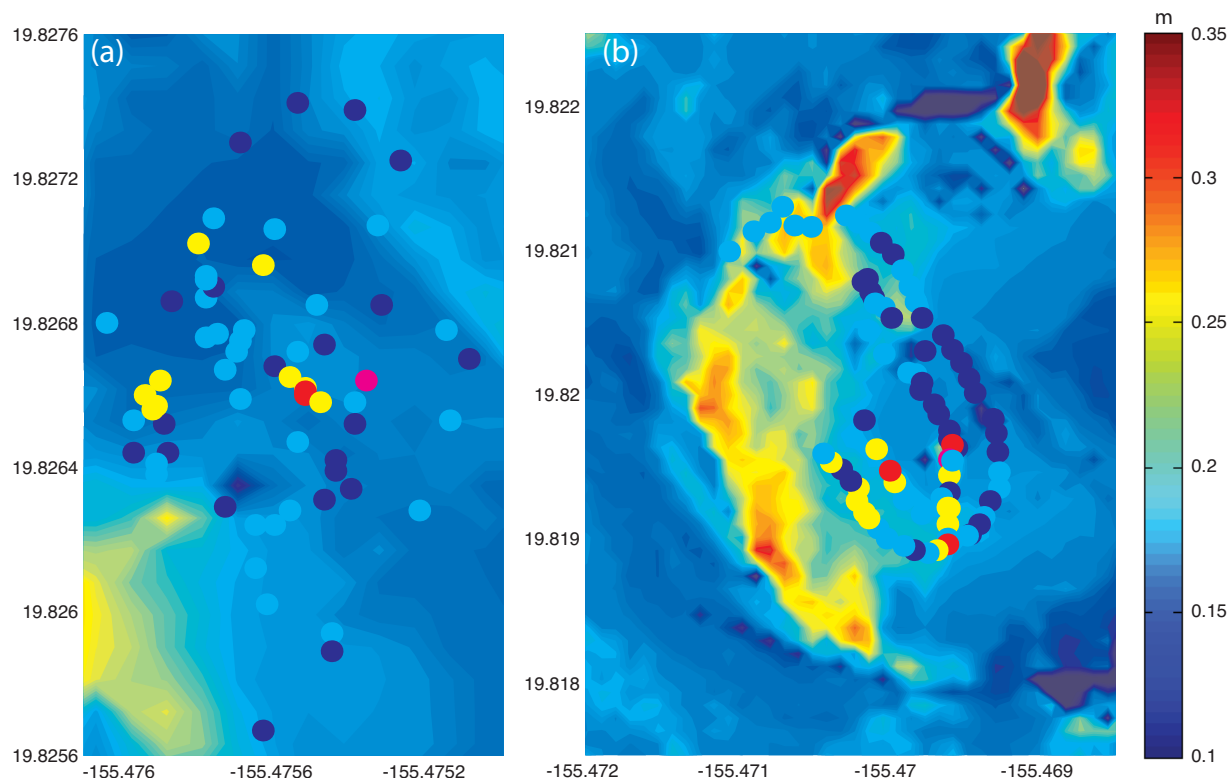


FIGURE 6. (a) Pu'u Hau'oki, and (b) Pu'u Wēkiu modeled snow depth (color contours in m) for 0959 UTC 11 January 2011; snow depth observations (colored dots) between 2130 UTC 11 January and 0000 UTC 12 January 2011.

Winds during snow events for 2009 are predominantly westerly (Fig. 7, part b). January, March, and November have the greatest variation in snow event wind direction. In November, there are a number of events with average winds being northerly. In January and March there are a number of snow events having easterly winds. The higher percentages of northeasterly and southeasterly winds are not seen during snow events for 2009, as they were in 2008. Winds with strong northern and southern directions are also less frequent during snow events. Snowfall on the summit was recorded during 52 days out of the year for 2009 (Fig. 1, part b). Due to equipment failures, precipitation measurements from 2010 were limited.

In this study, it is suggested that bug fall accumulation patterns are governed by similar physics as snow transport. In estimating the long-term climatology of the bug-fall distribution, wind data (Fig. 8) and model results throughout the entire period of study were integrated. The modeled bug-fall climatology was not limited to using only snowfall days; rather it incorporates available wind data from January 2008 to December 2010. The main scope of the study is to focus on climatology of wind-driven moisture and nutrient sources, independently.

In overview, analysis of all the summit surface winds for the period of study, 2008 through 2010, shows that winds favor easterly and westerly directions. The summit experiences winds with easterly components 59% of the time, with a westerly component 41% of the time (Fig. 8). Southerly and northerly winds occur relatively infrequently and tend to be lighter. In total, summit winds greater than 10 m s^{-1} occurred 31% of the time. Stronger winds favor southwesterly and east-northeasterly directions (Fig. 8).

IMPACT OF SUMMIT PU'US ON WIND SPEED AND DIRECTION

MicroMet was run to model the changes that occur to winds as they interact with the pu'u stippled summit. Cardinal and intercardinal (north, south, east, west, northeast, southeast, southwest, and northwest) wind fields of 7 m s^{-1} were initialized into MicroMet to display how the pu'us affect winds from a given direction (Figs. 9 and 10).

Pu'u Wēkiu had the greatest impact on the wind field for all eight directions. Winds with easterly components have the greatest positive wind speed changes on the pu'u (Fig. 9, part a). The outer eastern slope of Pu'u Wēkiu for these three scenarios (east, northeast, southwest) saw an increase in wind speeds by ~20%.

For both direct west and east winds, Pu'u Wēkiu caused more winds to flow south than north around the pu'u judging from wind directional changes (Fig. 10). Pu'u Hau'oki does not exhibit any great speed changes; however, approaching winds with a westerly component experience a greater directional change than winds with an easterly component (Fig. 10). Wind speed changes due to interaction with Pu'u Hau'oki are most recognizable from winds that have north and east components. The increase, however, is not as distinct as seen on Pu'u Wēkiu. Consistent with expectations, the center depressions for all three pu'us experience wind speeds that are ~40% slower than surrounding winds.

SNOWMODEL CLIMATOLOGY

Wind and precipitation data for 2008 and 2009 (Figs. 1 and 7) are used in model runs to estimate the climatological distribution of

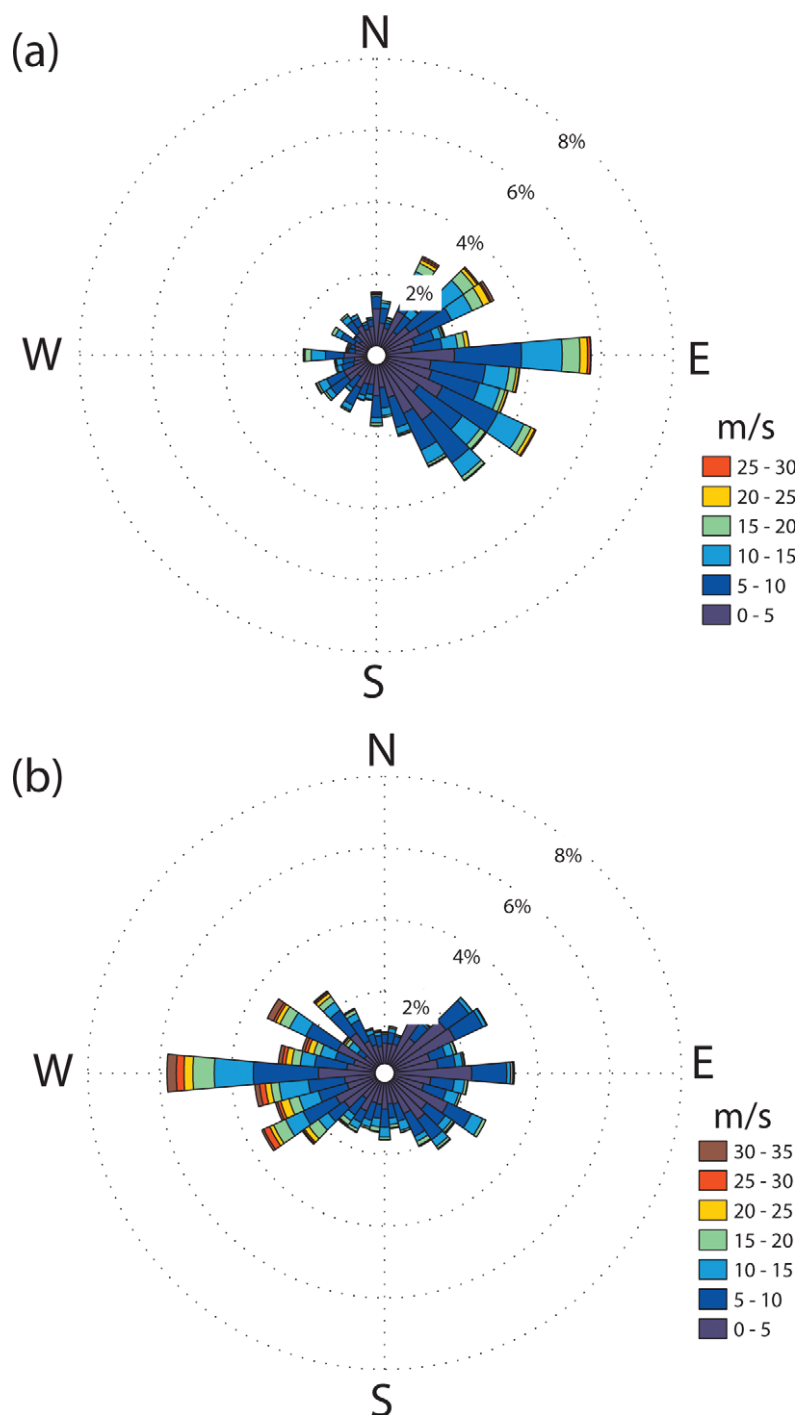


FIGURE 7. Wind rose of winds during snow events only for (a) 2008 and (b) 2009.

snowfall accumulation across the summit region. Precipitation data for 2010 are incomplete as a result of instrumentation issues. Therefore, the results for 2010 are not included in the snowfall climatology.

Accumulated snowfall and bug fall patterns complement each other (Figs. 11 and 12), with the maxima in accumulated snow and dead bugs on the lee sides of ridges and crests. Lower accumulation areas are seen on the windward sides in areas of enhanced winds, where saltation and scouring are active (Figs. 11 and 12). Differences in the patterns of bug-fall and snowfall accumulation are consistent with differences in the dominant wind direction over the days of integration.

Pu'u Haukea's maxima for snowfall and bug fall consistently

occur on the outer southern and southeastern slopes (Figs. 13, part a, and 14, part a). A second snowfall maximum is seen on the inner northeastern slope of Pu'u Haukea.

Pu'us Poli'ahu and Pōhaku display similar patterns for snowfall and bug fall (Figs. 13, part b, and 14, part b). Maxima are seen on the southern slopes of Pu'u Pōhaku and Pu'u Poli'ahu. The maxima associated with the lateral ridges on the southwest slope of Pu'u Poli'ahu are well defined. Pu'u Wēkiu and Pu'u Hau'oki clearly show the effect that wind direction and speed have on accumulation locations for both snow and bug fall (Figs. 13, part b, and 14, part b). Maxima on Pu'u Wēkiu are seen on both the inner and outer eastern slope and

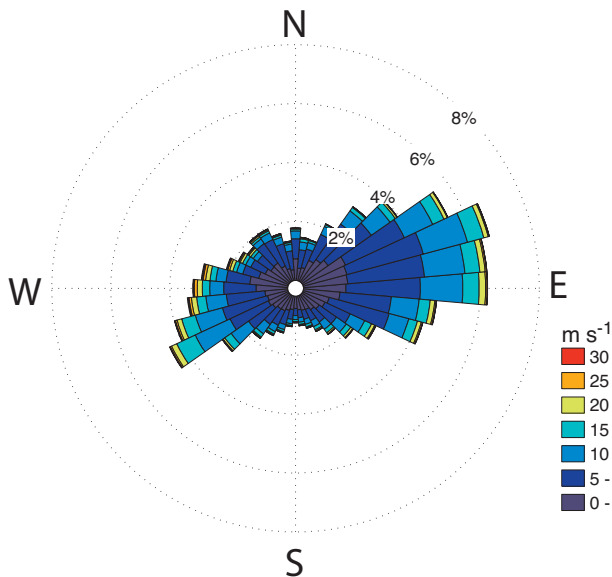


FIGURE 8. Wind rose for all Mauna Kea summit winds for January 2008 through December 2010.

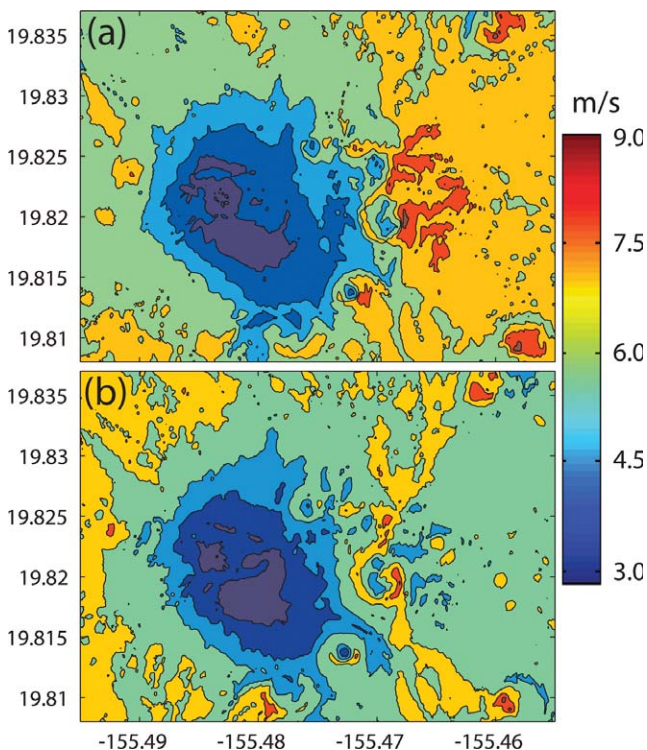


FIGURE 9. Modeled wind speed (m s^{-1}) from cardinal wind fields: (a) east, (b) west.

on either side of the ridge extending north from the pu'u. The higher values on the eastern slopes are the product of the higher westerly wind speeds observed in 2009. The outer southern slope in both easterly and westerly winds accumulates maxima on Pu'u Wēkiu.

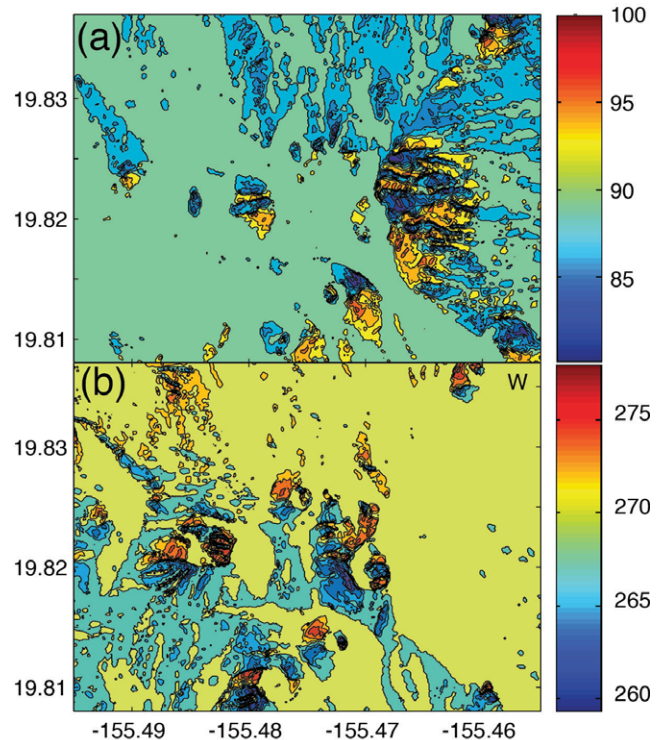


FIGURE 10. Modeled wind direction from cardinal wind fields: (a) east (90°), (b) west (270°).

Conclusions and Discussion

The summit of Mauna Kea is an eolian system, where nutrients primarily come from matter being blown in from lower elevations. The pu'u stippled summit area affects local wind patterns and summit deposition of moisture and nutrients, which is of great interest in understanding the life cycle, habitat, and distribution of the Wēkiu bug and other summit species. Pu'us protrude as much as 200 m above the surrounding surface elevations, creating slope angles of $\sim 30\%$ grade. In general, winds traveling up hills or pu'us and on the ridges are faster than those over flat terrain and within the pu'u center. Winds that travel around the pu'u at constant elevation also experience increases in speed. On the downslope sides, wind speeds tend to decelerate (Spalding, 1979). As the wind approaches the pu'us, it is forced around or over the pu'u.

For the summit of Mauna Kea, winds with an easterly or northerly direction produce the greatest acceleration in wind speed, especially on Pu'u Wēkiu, the largest cinder cone. Consequently, the maxima in accumulated snow and bug fall are seen on the lee sides of ridges and crests, where deposits are made as the wind falls below the thresholds for suspension or saltation. The results from this study are consistent with those found in Spalding's (1979) work on eolian ecology of the White Mountains in California. According to Spalding's work, largest deposits were found below a sharply defined section of the ridge where the leeward effect is the greatest.

Areas like Pu'u Haukea and Pu'u Poli'ahu have the greatest snowfall accumulation on their southern outer slopes. The summation of the years creates a smoother gradient of snow along the

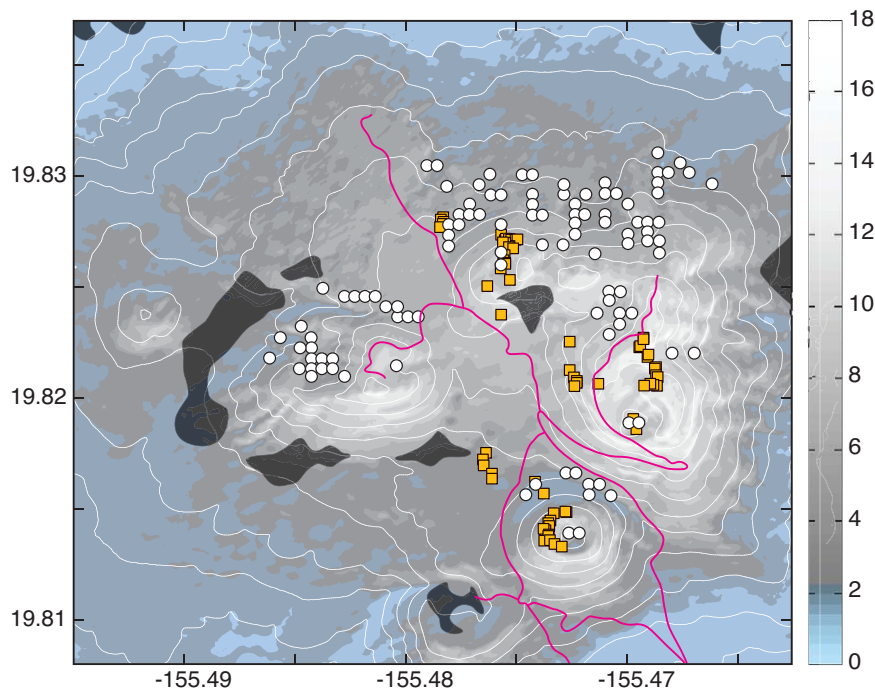


FIGURE 11. Modeled snow depth (in meters, shading) and elevation (white contours) of Mauna Kea summit for the 2-year total from 2008 to 2009, and Wēkiu Bug trap locations from 2002 to 2008 with positive capture rates (yellow boxes), locations with extended subfreezing temperatures (white circles). Red lines indicate roads and dark shading indicates areas of lava flows and glacial till found to be unsuitable as Wēkiu bug habitat (Lockwood, 2000).

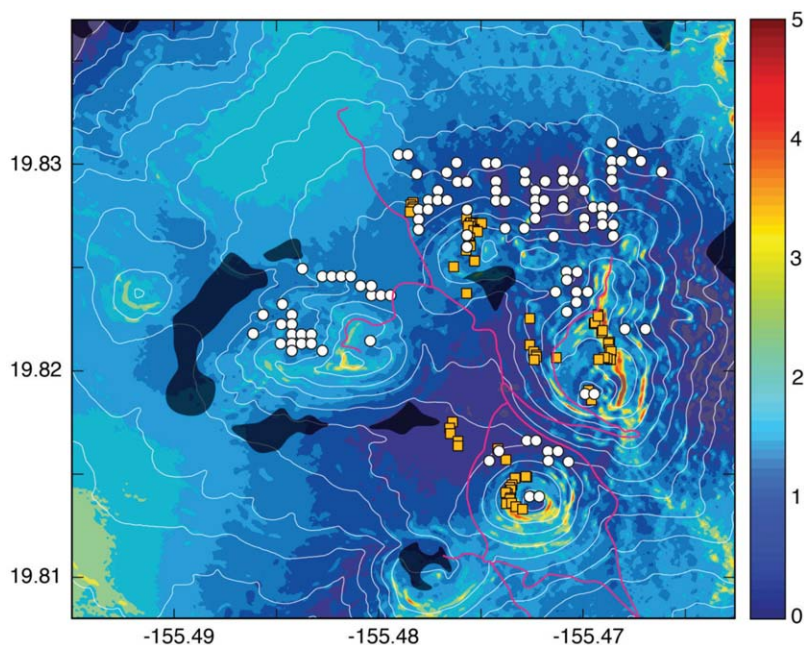


FIGURE 12. As in Figure 11, but for modeled bug fall density (undefined relative scale, colored shading) on Mauna Kea for 3-year total from 2008 through 2010.

slope, as the percentage of east to west winds between the two years becomes comparable.

This study uses the assumption that bug fall transport is governed by similar physics as snow transport, with allowances made for the fact that bug fall does not change phase. The modeled maxima in bug-fall accumulation is located on the leeward sides of the pu'us, and the position of the maxima is controlled by wind speed, much like that of the snowfall accumulation. The case study suggests that the model may have a tendency to underestimate the wind speed, and snow may actually extend further down the slope

on the leeward side. As expected, lower accumulation is seen on the windward sides in areas of enhanced winds, where saltation and scouring are active.

SPECIFIC CONCLUSIONS

The center depressions for the three main pu'us experience wind speeds that are ~40% slower than surrounding winds.

Prevailing easterlies have maximum moisture and nutrient accumulations on the inner eastern slope and the outer western slope

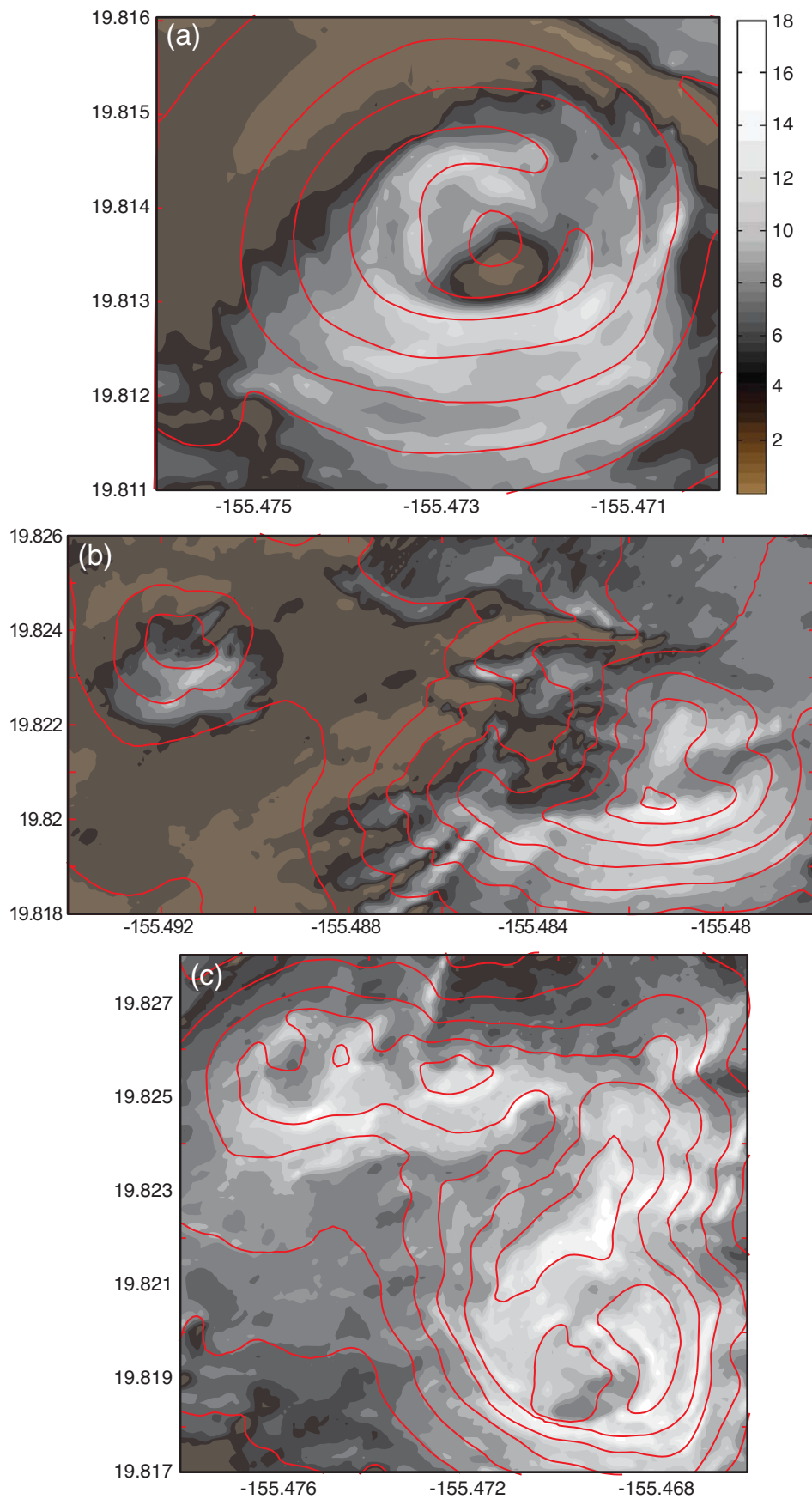


FIGURE 13. Same as Figure 11, but with elevation contours in red, but for (a) Pu'u Haukea; (b) Pu'u Pōhaku and Pu'u Poli'ahu; and (c) Pu'u Hau'oki and Pu'u Wēkiu.

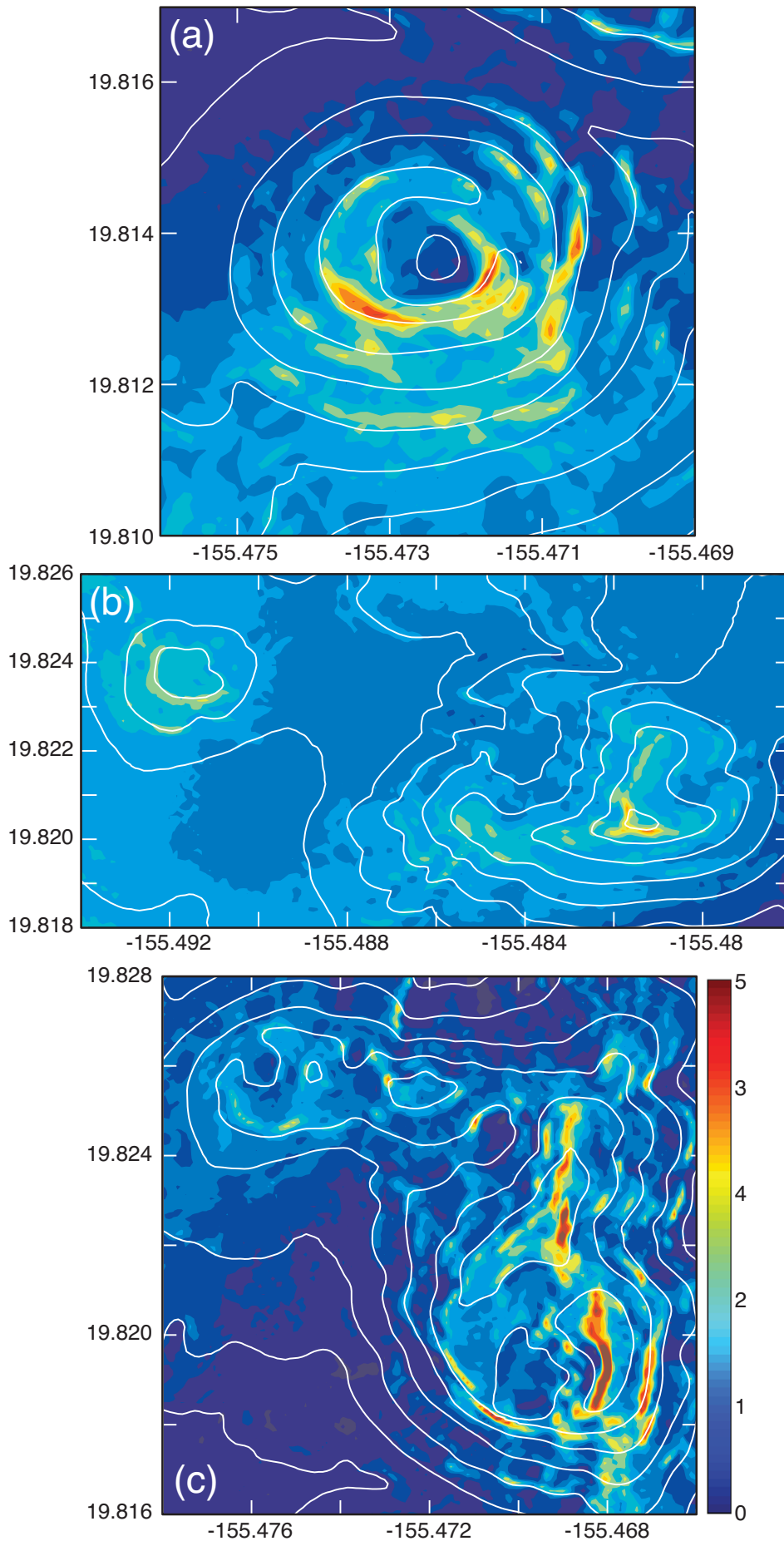


FIGURE 14. Same as Figure 12, but for (a) Pu'u Haukea; (b) Pu'u Pōhaku and Pu'u Poli'ahu; and (c) Pu'u Hau'oki and Pu'u Wēkiu.

TABLE 3

Summary of 2004–2011 Wēkiu bug expeditions conducted on Mauna Kea under the Hawaii Biological Survey.

Year	Total bug count ¹	Total trap days ²	Total traps
April 2004	14	10	5
July 2004	1	264	50
May 2005	31	529	90
June 2005	39	382	63
April 2006	13	454	70
May 2006	85	594	88
June 2007	537	252	42
July 2008	70	120	30
July 2009	118	285	45
June 2010	3047	300	50
June 2011	3084	300	50
Totals	7039	3490	583

¹Total Bug count = number of Wēkiu bugs counted between traps and visual observations.

²Total Trap Days = summation of total nights x total number of traps per site.

on Pu'u Wēkiu and the ridge extending north from the pu'u. The highest nutrient concentrations are toward the upper portion of the slope. Stronger winds cause nutrients to also accumulate on the outer northwestern slope of Pu'u Wēkiu.

Prevailing westerlies allow for moisture and nutrients to collect along the inner western slope of Pu'u Wēkiu. Moisture and nutrient accumulation is the greatest on the outer eastern slope of Pu'u Wēkiu, with the nutrient maxima accumulating half way up this side. Additionally, the eastern slope of the ridge extending from Pu'u Wēkiu traps nutrients on the upper portion of the slope.

Pu'u Pōhaku's maxima of nutrients and moisture occur on the outer southern slope. There is a second bug-fall maxima on the western slope.

Nutrient and moisture supplies on Pu'u Haukea are the greatest on the outer southern and southeastern slopes and the inner northwestern slope.

Maximum moisture on Pu'u Poli'ahu is found continuously down the outer southern slope. Nutrient accumulation occurs mainly on the upper section of the outer southern slope. Down the inner northern slope, nutrient and moisture maxima occur.

Nutrient accumulation on Pu'u Hau'oki is minimal, with moisture accumulation occurring on the outer southern slope.

DISCUSSION

The synoptic-scale winds on the summit are mainly controlled by the prevailing surface high-pressure center that is located north of the Hawaiian Islands and the position of the polar jet stream and its storm track, which shifts southward in winter. When the high pressure dominates, the winds favor easterly directions, and when the jet stream expands near Hawaii, the winds turn westerly. The location of both the high and the jet are influenced by ENSO. On the local scale, the variable terrain of the surface alters the free atmosphere wind significantly.

Wind specifics are important in describing summit life, which is fully sustained through an eolian system. The strength and direction of the wind is important in determining how much snow and nutrient are carried and where they are eventually deposited. An increase in wind speed increases the saltation and turbulent suspension and results in the moisture and nutrient maxima accumulating farther down the slope of an associated pu'u. Slope angle and aspect have primary effects on wind speed and direction, and subtle secondary effects on the accumulation patterns.

The variables used to simulate incoming bug fall are hypothetical and are set at the minimum solid precipitation value for the model to run. It is suggested that wind is the primary agent of debris transportation.

It is believed that a primary source for the bug fall is from the tundra and brush areas just below the summit area and above the treeline, with some additional bugs coming from agricultural areas farther from the summit (Jesse Eiben, personal communication). Trapping efforts performed in September 2002 by Englund et al. (2002) found high concentrations of eolian drift around the alpine zone. Their research suggests greener and wetter conditions above 1200 m contribute to the high concentrations of eolian debris on the summit. Within three days, various traps around the summit had bug-fall accumulations between 0.6 and 1.3 cm. However, trapping efforts in 2001 and April/May 2002 did not experience similar magnitude of eolian drift. Guppy (1897) found the greatest amounts of eolian debris on Mauna Loa occur with southerly winds.

For modeling purposes, background bug fall from the perimeter of the study area is initially evenly distributed. Comprehensive time-series data on bug fall with analysis of the taxonomy and source of the bugs are not available, as they can be very time consuming and expensive to obtain. Since the conclusion of this study, annual summit surveys by Englund et al. (2012) and Preston et al. (2012) have documented the makeup of eolian debris found on various pu'us. However, the ability to validate the bug fall model results quantitatively remains very limited at this time. Studies have yet to include eolian debris incoming volume. Nevertheless, we argue that the bug fall results are of interest, because they provide a potentially useful guide to entomologists in the field working to locate areas of potential food sources for the scavenger Wēkiu bug populations.

The rotation of synoptic wind from prevailing easterlies (summer) to more variable easterlies and westerlies (winter) affects accumulation patterns on the summit, with the greatest differences occurring on Pu'u Wēkiu. Western wind regimes deposit most nutrients on the outer eastern slopes of the pu'u, whereas during easterly wind regimes, the outer western and the inner eastern slopes of Pu'u Wēkiu accumulate the most nutrients. Nutrients are found on the outer southern slope of Pu'u Wēkiu in both easterly and westerly winds.

Bug-fall and snowfall fields show similar deposition patterns, but the fields are not exact replicas due to the different set of days used in the integration. The bug-fall accumulations were modeled using winds from the entire three-year period. For snowfall, only the winds that were present during snow events were used to distribute snowfall on the summit. Also, sublimation and melting are ignored when modeling bug fall; there are no losses to the maxima accumulations through phase changes. Nutrient maxima occur in clumped areas, while snowfall accumulation areas are more continuous down the slope. This clumping of maxima bug-fall areas may arise from the uniform larger size distribution of the bug fall.

Several field surveys have helped to identify the locations favorable for Wēkiu bug habitat through various trapping techniques (Brenner, 2006; Englund et al., 2002, 2005, 2006, 2007, 2009, 2010, 2012; Eiben and Rubinoff, 2010; Preston et al., 2012). Wēkiu bugs have been recorded on the west and northwest rim of Pu'u Haukea, in the flatter area between Pu'u Haukea and Pu'u Poli'ahu, on the northern side of Pu'u Hau'oki and on the southern and eastern rim, on the outer western slope of Pu'u Wēkiu, in the Pu'u Wēkiu center depression, on the inner eastern slope of Pu'u Wēkiu, and on the outer eastern slope of Pu'u Wēkiu and the ridge extending from the pu'u (Figs. 11 and 12).

The Hawaii Biological Surveys have led Wēkiu bug field expeditions since 2002 (Englund et al., 2002, 2005, 2006, 2007, 2009, 2010, 2012; and Preston et al., 2012). Polhemus (2001) did an initial study on Pu'u Haukea in 2001. Within these expeditions, several traps are placed around the summit, mainly focusing on locations including Pu'u Haukea, Pu'u Hau'oki, Pu'u Wēkiu, near the VLBA (Very Long Baseline Array) site, Pu'u Pohaku, Pu'u Poliahu, and the Poi Bowl. Generally, the expeditions take place in late spring to early summer with traps being on the slopes for a week at a time. Between 2004 and 2011, 7039 Wēkiu bugs were counted between all sites and traps, this includes Wēkiu bugs in traps and visually observed (Table 3).

The model output shows that the locations of the Wēkiu bug recordings and trappings, except for the area between Pu'u Haukea and Pu'u Poli'ahu and the center depression of Pu'u Wēkiu, receive high amounts of snowdrift over the winter season. The locations that receive high snowdrifts also accumulate the highest density bug fall, except for Pu'u Hau'oki. Bug fall accumulation is considerably less on Pu'u Hau'oki than Pu'u Haukea or Pu'u Wēkiu.

The pu'us are cinder cones and are made up of ash, lapilli, and cinder from explosions that occurred on the summit. This combination of volcanic rock allows for large interstitial areas between rocks to occur, a necessity for the Wēkiu bug. The majority of the land surrounding the pu'us is composed of older hawaiite-mugearite lava flows, which is primarily made up of 'a'ā lava with large rough sections. The geological makeup surrounding Pu'u Pōhaku's base is primarily glacial till, as well as the eastern side of Pu'u Wēkiu. The finer makeup of glacial till is unsuitable for Wēkiu bug life (Englund et al., 2002; Eiben and Rubinoff, 2010).

The pu'us on the summit act to speed up and slow down winds, change their direction, and thereby act as a trap for moisture and nutrients being blown on the summit. Concurrently, the pu'us are generally areas with high interstitial spaces (like cinder), which is the preferred habitat for the Wēkiu bug. The combination of moisture, nutrients, and cinder substrate is presumably where the population of Wēkiu bugs will be found. Previous trapping locations support this suggestion (Figs. 11 and 12). It is hoped that the results of the snow and bug-fall climatology presented in this paper will be of value to entomologists and biologists in their efforts to better understand and characterize the fragile ecology of the summit area of Mauna Kea.

Acknowledgments

Foremost, we are indebted to Dr. Glen Liston for giving us access to his SnowModel and for his helpful comments and support throughout this research. We are grateful to Sara da Silva for help with data analysis tools. Thanks go to Ryan Lyman for his efforts in siting and collecting the Davis weather station data. Lyman, along with Chris Chambers and Matt Foster helped to collect case

snow depth measurements. This research was supported by the Office of Mauna Kea Management.

References Cited

- Anderson, E. A., 1976: *A Point Energy and Mass Balance Model of a Snow Cover*. Washington, D.C.: NOAA Technical Report NWS-19, 150 pp.
- Ashlock, P., and Gagne, W., 1983: A remarkable new *Micropterous nysius* species from the aeolian zone of Mauna Kea, Hawaii Island (Hemiptera: Lygaeidae). *International Journal of Entomology*, 25: 47–55.
- Barnes, S. L., 1973: Mesoscale objective analysis using weighted time-series observations. Norman, Oklahoma: National Severe Storms Laboratory, NOAA Tech Memo ERL NSSL-62, 60 pp. Accession number NTIS-COM-73-10781.
- Bely, P.-Y., 1987: Weather and seeing on Mauna Kea. *Publications of the Astronomical Society of the Pacific*, 99: 569–570.
- Blumenstock, D. I., and Price, S., 1967: *Climates of the states: Hawaii*. Washington, D.C.: U.S. Department of Commerce, Climatology of the US, No. 60-51, 27 p.
- Brenner, G. J., 2006: Wēkiu Bug Baseline Monitoring. Quarterly Report, 4th Quarter 2006. A Technical Report Prepared for the W. M. Keck Observatory.
- Bryan, E. H., Jr., 1923: Insects from the Summit of Mauna Kea. *Proceedings of the Hawaii Entomology Society*, 5: 287–288.
- Bryan, E. H., Jr., 1926: Additional notes on the insects occurring on Mauna Kea and Mauna Loa. *Proceedings of the Hawaii Entomology Society*, 6: 280–282.
- Cao, G., Giambelluca, T. W., Stevens, D. E., and Schroeder, T. A., 2007: Inversion variability in the Hawaiian trade wind regime. *Journal of Climate*, 20: 1145–1160.
- da Silva, S. C., 2006: *Climatological Analysis of Meteorological Observations at the Summit of Mauna Kea*. University of Hawaii at Mānoa, Department of Meteorology, OMKM Technical Report, 77 pp. Available at <http://www.mkwc.ifa.hawaii.edu/archive>.
- da Silva, S. C., 2012: *High Altitude Climate of the Island of Hawai'i*. M.S. thesis, Department of Meteorology, University of Hawaii at Mānoa, 110 pp. Available at www.soest.hawaii.edu/MET/Faculty/businger/highlights.html.
- Ehse, J., 2007: *GIS-gestützte Abschätzung möglicher Permafrostvorkommen am Mauna Kea, Hawaii, mittels klimageographischer Modellierung*. M.A. thesis, Department of Geography and Climate, Rheinisch-Westfälische Technische Hochschule University–Aachen, 106 pp.
- Eiben, J., and Rubinoff, D., 2010: Life history and captive rearing of the Wēkiu bug (*Nysius wēkiuicola*, Lygaeidae), an alpine carnivore endemic to the Mauna Kea volcano of Hawaii. *Journal of Insect Conservation*, 14: 701–709.
- Englund, R. A., Polhemus, D. A., Howarth, F. G., and Montgomery, S. L., 2002: *Range, Habitat, and Ecology of the Wēkiu Bug (Nysius weikiuicola), A Rare Insect Species Unique to Mauna Kea, Hawaii Island*. Report prepared for Office of Mauna Kea Management, University of Hawaii at Hilo, Contribution No. 2002-023 to the Hawaii Biological Survey.
- Englund, R. A., Ramsdale, A., McShane, M., Preston, D. J., Miller, S., and Montgomery, S. L., 2005: *Results of the 2004 Wēkiu Bug (Nysius weikiuicola) Surveys on Mauna Kea, Hawaii Island*. Hawaii Biological Survey final report prepared for Office of Mauna Kea Management, University of Hawaii at Hilo. Contribution No. 2005-003 to the Hawaii Biological Survey.
- Englund, R. A., Vorsino, A. E., Laederich, H. M., Ramsdale, A., and McShane, M., 2006: *Results of the 2005 Wēkiu Bug (Nysius weikiuicola) Surveys on Mauna Kea, Hawaii Island*. Hawaii Biological Survey final report prepared for Office of Mauna Kea Management, University of Hawaii at Hilo, Contribution No. 2006-010 to the Hawaii Biological Survey.

- Englund, R. A., Vorsino, A. E., and Laederich, H. M., 2007: *Results of the 2006 Wēkiu Bug (Nysius weikiuicola) Surveys on Mauna Kea, Hawaii Island*. Hawaii Biological Survey final report prepared for Office of Mauna Kea Management, University of Hawaii at Hilo, Contribution No. 2007-003 to the Hawaii Biological Survey.
- Englund, R. A., Preston, D. J., Vorsino, A. E., Evenhuis, N. L., Myers, S., and Englund, L. L., 2009: *Results of the 2007–2008 Alien Arthropod Species and Wēkiu Bug monitors on Mauna Kea, Hawaii Island*. Hawaii Biological Survey final report prepared for Office of Mauna Kea Management, University of Hawaii at Hilo, Contribution No. 2009-004 to the Hawaii Biological Survey.
- Englund, R. A., Preston, D. J., Myers, S., Englund, L. L., Imada, C., and Evenhuis, N. L., 2010: *Results of the 2009 Alien Species and Wēkiu Bug (Nysius weikiuicola) Surveys on the Summit of Mauna Kea, Hawaii Island*. Hawaii Biological Survey final report prepared for Office of Mauna Kea Management, University of Hawaii at Hilo, Contribution No. 2010-013 to the Hawaii Biological Survey.
- Englund, R. A., Preston, D. J., Myers, S., Imada, C., and Englund, L., 2012: *Results of the 2010 Alien Species and Wēkiu Bug (Nysius weikiuicola) Surveys on the Summit of Mauna Kea, Hawaii Island*. Hawaii Biological Survey final report prepared for Office of Mauna Kea Management, University of Hawaii at Hilo, Contribution No. 2012-002 to the Hawaii Biological Survey.
- Fish and Wildlife Service, 2010: Endangered and Threatened Wildlife and Plants; Review of Native Species That are Candidates for Listing as Endangered or Threatened; Annual Notice of Findings on Resubmitted Petitions; Annual Description of Progress on Listing Action. 50 CFR Part 17, Docket No. FWS-R9-ES-2010-0065; MO-9221050083-B2.
- Greene, E. M., Liston, G. E., and Pielke, R. A., Sr., 1999: Simulation of above treeline snowdrift formation using a numerical snow-transport model. *Cold Regions Science and Technology*, 30: 135–144.
- Group 70 International, 2000: *Mauna Kea Science Reserve Master Plan: A final environmental impact statement Master Plan*. Report prepared for Research Corporation of the University of Hawai'i by Group 70 International, Honolulu.
- Guppy, H. B., 1897: The summit of Mauna Loa. *Nature*, 57: 20–21.
- Hartt, C. E., and Neal, M. C., 1940: The plant ecology of Mauna Kea Hawaii. *Ecology*, 21: 237–266.
- Jackson, P. S., and Hunt, J. C. R., 1975: Turbulent wind flow over a low hill. *Quarterly Journal of the Royal Meteorological Society*, 101: 929–955.
- James, P. E., 1922: Koppen's classification of climates: a review. *Monthly Weather Review*, 50: 69–72.
- Kind, R. J., 1981: Snow drifting. In Gray, D. M., and Male, D. H. (eds.), *Handbook of Snow, Principles, Processes, Management, and Use*. Oxford: Pergamon Press, 338–359.
- Koch, S. E., DesJardins, M., and Kocin, P. J., 1983: An interactive Barnes objective map analysis scheme for use with satellite and conventional data. *Journal of Climate and Applied Meteorology*, 22: 1487–1503.
- Kodama, K. R., and Businger, S., 1998: Weather and forecasting challenges in the Pacific region of the National Weather Service. *Weather and Forecasting*, 13: 523–546.
- Kosugi, K., Nishimura, N., and Maeno, N., 1992: Snow ripples and their contribution to the mass transport in drifting snow. *Boundary Layer Meteorology*, 59: 59–66.
- Liston, G. E., and Elder, K., 2006a: A meteorological distribution system for high-resolution modeling (MicroMet). *Journal of Hydrometeorology*, 7: 217–234.
- Liston, G. E., and Elder, K., 2006b: A distributed snow-evolution modeling system (SnowModel). *Journal of Hydrometeorology*, 7: 1259–1276.
- Liston, G. E., and Sturm, M., 1998: A snow-transport model for complex terrain. *Journal of Glaciology*, 44: 498–516.
- Liston, G. E., and Sturm, M., 2002: Winter precipitation patterns in Arctic Alaska determined from a blowing snow model and snow-depth observations. *Journal of Hydrometeorology*, 3: 646–659.
- Liston, G. E., and Sturm, M., 2006: A meteorological distribution system of high-resolution terrestrial modeling (MicroMet). *Journal of Hydrometeorology*, 7: 217–234.
- Liston, G. E., Haehnel, R. B., Sturm, M., Hiemstra, C. A., Berezovskaya, S., and Tabler, R. D., 1998: Instruments and methods, simulating complex snow distributions in windy environments using SnowTran-3D. *Journal of Glaciology*, 53: 241–256.
- Liston, G. E., Winther, J.-G., Bruland, O., Elvehoy, H., Sand, K., and Karlof, L., 2000: Snow and blue-ice distribution patterns on the coastal Antarctic ice sheet. *Antarctic Science*, 12: 69–79.
- Liston, G. E., Haehnel, R. B., Sturm, M., Hiemstra, C. A., Berezovskaya, S., and Tabler, R. D., 2007: Simulating complex snow distributions in windy environments using SnowTran-3D. *Journal of Glaciology*, 53: 241–256.
- Marsh, P., 1999: Snowcover formation and melt: recent advantages and future prospects. *Hydrological Processes*, 13: 2117–2134.
- Papp, R. P., 1981: High altitude aeolian ecosystems in the Hawaiian Islands. *Proceedings of the Third Conference in Natural Sciences, Hawaii Volcanoes National Park, Coop. Natl. Pk. Resources Studies Unit*. University of Hawaii at Mānoa, Department of Botany: 259–264.
- Polhemus, D. A., 2001: A preliminary survey of Wēkiu bug populations on Pu'u Hau Kea in the Mauna Kea Ice Age Natural Reserve, Hawaii Island, Hawaii. In Englund, R. A., Polhemus, D. A., Howarth, F. G., and Montgomery, S. L., 2002: Range, Habitat, and Ecology of the Wēkiu Bug (*Nysius weikiuicola*). A Rare Insect Species Unique to Mauna Kea, Hawai'i Island. Washington, D.C.: Smithsonian Institution, Department of Systematic Biology report for the Natural Area Reserve System. Report prepared for Office of Mauna Kea Management, University of Hawaii at Hilo. Contribution No. 2002-023 to the Hawaii Biological Survey.
- Pomeroy, J. W., and Gray, D. M., 1990: Saltation of snow. *Water Resources Research*, 26: 1583–1594.
- Porter, S. C., 1997: Late Pleistocene aeolian sediments related to pyroclastic eruptions of Mauna Kea Volcano, Hawaii. *Quaternary Research*, 47: 261–276.
- Prasad, R., Tarboton, D. G., Liston, G. E., Luce, C. H., and Seyfried, M. S., 2001: Testing a blowing snow model against distributed snow measurements at Upper Creek, Idaho, United States of America. *Water Resources Research*, 37: 1341–1350.
- Preston, D. J., Englund, R. A., Myers, S., Imada, C., and Garcia, J., 2012: *Results of the 2011 Alien Species and Wēkiu Bug (Nysius weikiuicola) Surveys on the Summit of Mauna Kea, Hawaii Island*. Hawaii Biological Survey final report prepared for Office of Mauna Kea Management, University of Hawaii at Hilo, Contribution No. 2012-016 to the Hawaii Biological Survey.
- Schmidt, R. A., 1982: Vertical profiles of wind speed, snow concentration, and humidity in blowing snow. *Boundary Layer Meteorology*, 23: 223–246.
- Spalding, J. B., 1979: The aeolian ecology of White Mountain Peak, California: windblown insect fauna. *Arctic and Alpine Research*, 11: 83–94.
- Sustainable Resources Group International, 2009: Natural resources management plan for the UH management areas on Mauna Kea: A sub-plan of the Mauna Kea Comprehensive Management Plan. Prepared by the Sustainable Resources Group Internationals, Kailua, Hawaii.
- Swan, L., 1963: Aeolian zone. *Science*, 140: 77–78.
- Ugolini, F. C., 1974: Hydrothermal origins of the clays from the upper slopes of Mauna Kea, Hawaii. *Clay and Clay Minerals*, 22: 189–194.
- Whiteman, C. D., 2000: *Mountain Meteorology—Fundamentals and Applications*. New York: Oxford University Press.
- Wolfe, E. W., Wise, W. S., and Dalrymple, G. B., 1997: *The Geology and Petrology of Mauna Kea Volcano, Hawaii—A Study of Post Shield Volcanism*. Reston, Virginia: U.S. Geological Survey Professional Paper 1557, 143 pp.
- Woodcock, A. H., 1974: Permafrost and climatology of a Hawaii volcano crater. *Arctic and Alpine Research*, 6: 49–62.
- Worthley, L. E., 1967: *Weather Phenomena in Hawaii. Part I. Synoptic Climatology of Hawaii*. Hawaii Institute of Geophysics, University of Hawaii, 40 pp. Available from Dept. of Meteorology, University of Hawaii, 2525 Correa Road, Honolulu, Hawaii 96822.

MS accepted September 2014